Fundamental Battery Studies
Final Report

Subcontractor Report
prepared by

J. B. Goodenough
Center for Materials Science and Engineering
The University of Texas at Austin

January 2002

IAT.R 0274

Institute for Advanced Technology
The University of Texas at Austin

IAT

20020326 203

REPORT DOCUMENTATION PAGE

1. AGENCY USE ONLY (Leave blank)	2. REPORT DATE	3. REPORT TYPE AND DATES COVERED
	January 2002	technical report, 2001

4. TITLE AND SUBTITLE	5. FUNDING NUMBERS
Fundamental Battery Studies Final Report	Contract # DAAD17-01-D-0001

6. AUTHOR(S)

J. B. Goodenough (Center for Materials Science and Engineering, The University of Texas at Austin)

7. PERFORMING ORGANIZATION NAME(S) AND ADDRESS(ES)	8. PERFORMING ORGANIZATION REPORT NUMBER
Institute for Advanced Technology The University of Texas at Austin 3925 W. Braker Lane, Suite 400 Austin, TX 78759-5316	IAT.R 0274

9. SPONSORING / MONITORING AGENCY NAME(S) AND ADDRESS(ES)	10. SPONSORING / MONITORING AGENCY REPORT NUMBER
U.S. Army Research Laboratory ATTN: AMSRL-WM-B Aberdeen Proving Ground, MD 21005-5066	

11. SUPPLEMENTARY NOTES

12a. DISTRIBUTION / AVAILABILITY STATEMENT	12b. DISTRIBUTION CODE
Approved for public release; distribution unlimited.	A

13. ABSTRACT (Maximum 200 words)

The objectives of this grant were (1) to analyze the data taken by the Army Research Laboratory (ARL) on the operation of a Saft lithium-ion battery system being developed for pulsed-power applications, (2) to suggest an experimental strategy for determining the relative contributions of electronic and ionic processes in the initial discharge so that a decision could be made either to stop the project or to understand how to optimize performance, and (3) in the absence of feedback from Saft, to pursue an investigation of alternative cathode materials for lithium-ion batteries.

14. SUBJECT TERMS	15. NUMBER OF PAGES
pulsed power, Saft battery, battery design, lithium-ion battery	15
	16. PRICE CODE

17. SECURITY CLASSIFICATION OF REPORT	18. SECURITY CLASSIFICATION OF THIS PAGE	19. SECURITY CLASSIFICATION OF ABSTRACT	20. LIMITATION OF ABSTRACT
Unclassified	Unclassified	Unclassified	UL

INTENTIONALLY LEFT BLANK.

Contents

List of Figures

INTENTIONALLY LEFT BLANK.

FUNDAMENTAL BATTERY STUDIES

John B. Goodenough

INTRODUCTION

The objectives of this grant were (1) to analyze the data taken by the U.S. Army Research Laboratory (ARL) on the operation of a Saft lithium-ion battery system being developed for pulsed-power applications, (2) to suggest an experimental strategy for determining the relative contributions of electronic and ionic processes in the initial discharge so that a decision could be made either to stop the project or to understand how to optimize performance, and (3) in the absence of feedback from Saft, to pursue an investigation of alternative cathode materials for lithium-ion batteries.

THE PULSED-POWER APPLICATION

The Saft battery developers were attempting to optimize the short-time power delivered through a small-impedance load by a $Li_xC_6//Li_{1-x}CoO_2$ rechargeable battery. In this application, the battery should store both chemical and electrostatic energy. The open-circuit voltage of the battery approaches $V_{OC} \approx 4$ V, and the charge stored is $q = CV_{OC}$, where C is the capacitance of the battery. The charge q may be stored in the bulk of the anode or at the surface of the electrodes and current collectors. The initial current pulse on discharge would contain two components: one due to a capacitance of the current collectors and a rapid desorption of Li^+ ions from the anode surface and adsorption from the electrolyte to the cathode surface, and the other due to a slower insertion of Li^+ ions from the bulk of the anode to the electrolyte and from the electrolyte into the bulk of the cathode. In the first process, the battery acts as an ultracapacitor, and in the second, as a storage battery. In order to increase the capacitance C of the battery, the Saft developers were making the electrolyte thinner. However, a fundamental question for them was how to determine experimentally the fraction of the discharge current that comes from the faster process relative to the slower process so that they could test the effectiveness of changes in battery design.

SUGGESTED EXPERIMENTAL STRATEGY

The ARL had developed an equivalent circuit for the battery that allowed tracking of the terminal voltage with time on discharge into a small load impedance. The equivalent circuit contained capacitive and inductive elements, but it provided little insight as to how best to design the battery. We suggested the use of discharge pulses lasting a time Δt with a separation between pulses of $\Delta t'$, Fig. 1(a). A rapid drop $-\Delta V$ occurring in the time Δt would be followed by a recovery $+\Delta V'$ during $\Delta t'$, Fig. 1(b). The recovery $\Delta V'$ would

be due to bulk ionic processes, and the difference $|\Delta V - \Delta V'|$ would be a measure of the more rapid electronic processes. The Saft developers acknowledged that this was a good strategy, but there was no further feedback as to the results of their experiments.

We further pointed out that the electrodes of ultracapacitors are amorphous, those of batteries are crystalline. Since we are not in the business of optimizing battery fabrication, we left the problem with them and turned to studies of alternative cathode materials for lithium-ion batteries.

ALTERNATIVE CATHODE MATERIALS

Manganese Oxospinels

The oxospinel $Li_x[Mn_2]O_4$ has been extensively studied as an alternative to the layered $Li_{1-x}Co_{1-y}Ni_yO_2$ oxides because of cost considerations. In the range $0 < x < 1$, $Li_x[Mn_2]O_4$ gives a voltage $V \approx 4$ V vs. a Lithium anode; in the range $1 < x < 2.0$, it gives a $V \approx 3$ V. However, commercial realization has been frustrated by an irreversible capacity fading on cycling in both the 4-V and the 3-V ranges. A flat V vs. x curve in the 3-V range signals a wide two-phase domain between a cubic $x = 1.0$ and a tetragonal (c/a > 1) $x \approx 1.8$ phase; the Mn(III) concentration in the Li-rich $x \geq 1.8$ phase is high enough to induce a cooperative Jahn-Teller distortion of the spinel to tetragonal (c/a > 1) symmetry. The associated change in volume and symmetry tends to break up larger cathode particles on cycling, thus causing a capacity fade. Moreover, $Li[Mn_2]O_4$ in acidic (pH < 2.0) aqueous solution induces a surface disproportionation reaction $2Mn(III) = Mn(II) + Mn(IV)$ that is followed by dissolution of $Li^+ + Mn(II)$ to create λ-$MnO_2 = Li_\delta[Mn_2]O_4$ with $\delta \ll 1$. Therefore, the possibility that a similar disproportionation reaction may occur in a non-aqueous electrolyte is also a concern. Stabilization of the capacity of the electrode in the 3-V range could involve either the creation of particles of small size or a decoration of the surface with a molecule that would inhibit the surface disproportionation reaction.

In an attempt to decorate the surface of the particles with Cl^- ions, we prepared $Li[Mn_2]O_4$ by a mild sol-gel method in the presence of $MnCl_2 \cdot 4H_2O$. Although we had no Cl^- on the surface of the particles, we found that the capacity of our material was stable over many cycles across the two-phase region at temperatures up to 60°C. Apparently the disproportionation reaction was not a problem on discharge to 2.4 V. However, cycling in the 4-V range still exhibited a capacity fade, but the rate of fading decreased if the cathode was cycled through the 3-V range before returning to the 4-V range. Since some O_2 evolution has been observed at the top of the charge, i.e., at $V = 4.3$ V, we conjecture that octahedral-site Mn(IV) is oxidized to tetrahedral-site Mn(VI) with the loss of O_2, and the Mn(VI) that is not lost to the solution may be reduced back to octahedral-site Mn(III) on discharge in the 3-V range.

In order to understand the stability of our cathodes in the 3-V range, we examined our fabrication procedures for $Li[Mn_2]O_4$ prepared by the sol-gel method (SG-LMOS) and by

a conventional solid-state method (SS-LMOS). One step involved ball milling our powders, so we compared the X-ray diffraction (XRD) patterns of hand-ground samples (*e.g.*, SG-LMOSL) with samples that had been ball milled for t minutes (SG-LMOSt or SS-LMOSt). As can be seen in Fig. 2, the XRD peaks were increasingly broadened with ball milling time t. This increase could be due to a reduction in particle size and/or the introduction of lattice strain or stacking faults. The reciprocal-lattice breadths β^* of the unmilled powders were almost independent of $\sin\theta$, which indicates negligible lattice strain, whereas the ball-milled spinel powders were found to have a β^* strongly dependent on $\sin\theta$ and therefore to contain considerable lattice strain and/or stacking faults. Although the overall particle size was not greatly changed by the ball milling, TEM images and selected-area diffraction (SAD) patterns of the particles. Fig. 3, showed that ball milling created particles with many microdomains.
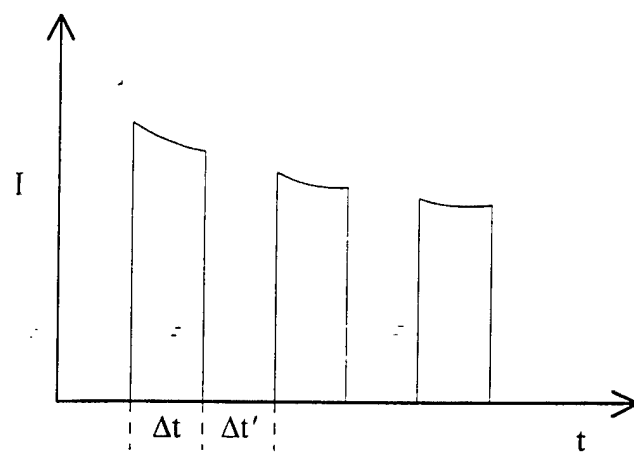
Thus by a simple step of ball milling the cathode particles for 1h, we have been able to stabilize our $Li_{1+x}[Mn_2]O_4$ ($0 < x < 1$) cathode materials against capacity fade in the 3-V range up to 60°C. as is illustrated by Figs. 4 and 5: the capacity increases with temperature for a given current density because of kinetic considerations. The capacity fade with increasing current density or reduced temperature is reversible.

$LiNaV_2(PO_4)_3$

We had previously investigated Lithium insertion into phosphates with the NASICON structure to determine the relative positions of the redox energies of the transition-metal M cations in the $M_2(PO_4)_3$ framework (Appendix A). The V(IV)/V(III) couple was found to give an attractive $V_{OC} = 3.7$ V versus a lithium anode. However, we were not able to prepare $Li_3V_2(PO_4)_3$ in the rhombohedral structure. To obtain the rhombohedral phase, it is necessary to begin with $Na_3V_2(PO_4)_3$ and ion exchange Li^+ for Na^+. This procedure gave us $Li_2NaV_2(PO_4)_3$. We decided to investigate whether the Na^+ ions interfere with the use of this material as a battery cathode. We found we could cycle lithium in and out reversibly; the displacement of some Na to the electrolyte did not cause a problem. The NASICON structure is an open framework that allows rapid diffusion of the Li^+ ions. The larger free volume for the Li^+ ions reduces the energy density for a standard battery, but if a rapid battery discharge is more important than the energy density, this structure has attractive features.

ACKNOWLEDGEMENT

Figure 1. Current vs. time and voltage vs. time profiles of a pulsed discharge.
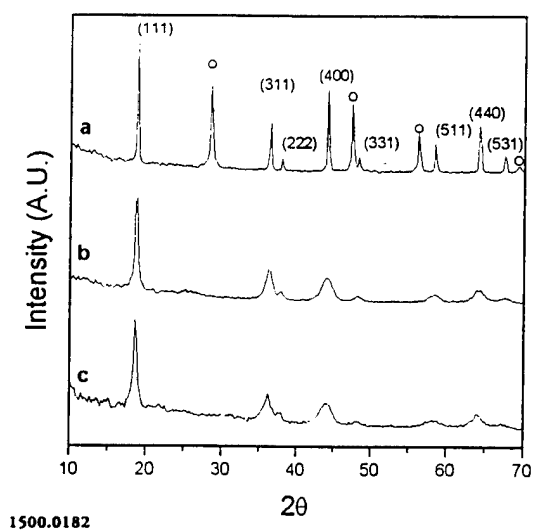
Figure 2. XRD patterns. (a) As-prepared, (b) after ballmilling for 60 min., and (c) after ballmilling for 120 min. Open circles denote Si internal standard.

4
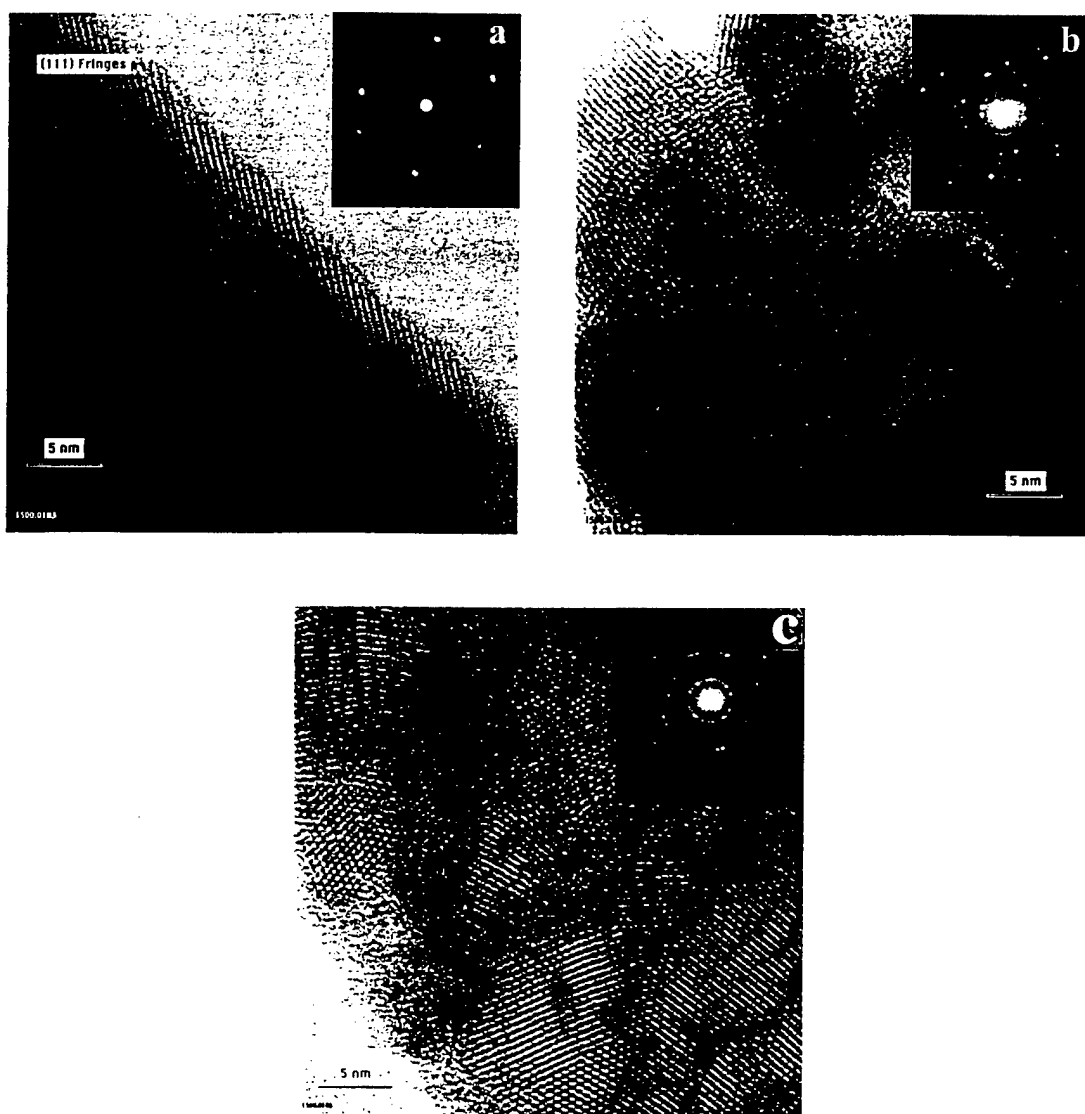
Figure 3. TEM images and electron diffraction patterns:
    (a) As prepared.
    (b) After ballmilling for 60 min.
    (c) After ballmilling for 120 min.
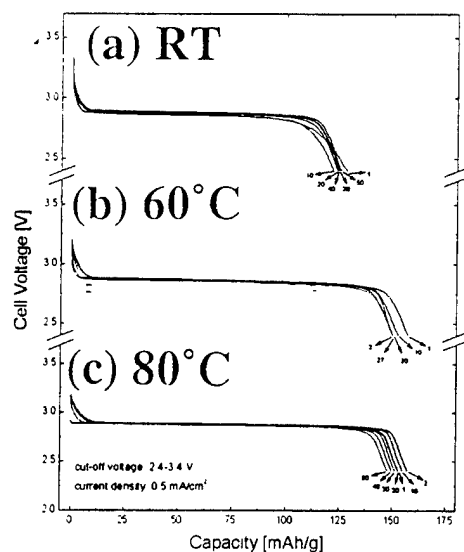
Figure 4. Discharge curves of $Li_{1.03}Mn_{1.91}O_4$ ballmilled for 60 min. in the voltage range of 2.4-3.4 at a current density of 0.5 mA/cm^2. (a) At room temperature (RT), (b) at 60°C, and (c) at 80°C.
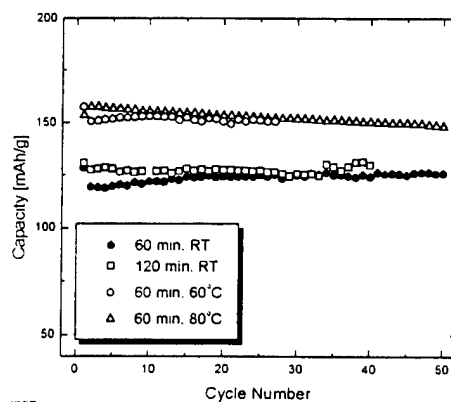
Figure 5. Discharge capacities of $Li_{1.03}Mn_{1.91}O_4$ ballmilled for 60 and 120 min. at RT, 60°C, and 80°C.

Distribution List

Administrator, Defense Technical
 Information Center
ATTN: DTIC-DDA
8725 John J. Kingman Road, Suite 944
Ft. Belvoir, VA 22060-6218

Director
U.S. Army Research Lab
ATTN: AMSRL OP SD TA
2800 Powder Mill Road
Adelphi, MD 20783-1145

Director
U.S. Army Research Lab
ATTN: AMSRL OP SD TL
2800 Powder Mill Road
Adelphi, MD 20783-1145

Director
U.S. Army Research Lab
ATTN: AMSRL OP SD TP
2800 Powder Mill Road
Adelphi, MD   20783-1145

Army Research Laboratory
AMSRL-CI-LP
Technical Library 305
Aberdeen Prvg Grd, MD 21005-5066

Dr. Mark Crawford
Institute for Advanced Technology
The University of Texas at Austin
3925 W. Braker Lane, Suite 400
Austin, TX 78759

Dr. Donald Eccleshall
Institute for Advanced Technology
The University of Texas at Austin
3925 W. Braker Lane, Suite 400
Austin, TX 78759

Dr. Harry Fair
Institute for Advanced Technology
The University of Texas at Austin
3925 W. Braker Lane, Suite 400
Austin, TX 78759

Dr. Marilyn Freeman
SAAL-ZT
Suite 9815
2511 Jefferson Davis Highway
Arlington, VA 22202

Charles Hummer
ARL
ATTN: AMSRL-WT-WD
Aberdeen Proving Ground, MD 21005-5066

Mr. Dennis Ladd
Commander, TACOM-ARDEC
Attn: AMSTA-AR-FSP-E / Dennis Ladd
Bldg. 354
Picatinny Arsenal, NJ 07806-5000

Tom Matty
Technology Concepts Management, Inc.
2400 Robbins Station
Irwin, PA 15642

Dr. Ian McNab
Institute for Advanced Technology
The University of Texas at Austin
3925 W. Braker Lane, Suite 400
Austin, TX 78759

Dr. Chadee Persad
Institute for Advanced Technology
The University of Texas at Austin
3925 W. Braker Lane, Suite 400
Austin, TX 78759

Distribution List

Dr. Jim Sarjeant
State University of New York at Buffalo
312 Bonner-Elect. Engr.
University at Buffalo - SUNY/AB
P. O. Box 601900
Buffalo, NY 14260-1900

Dr. Edward M. Schmidt
U.S. Army Research Laboratory
AMSRL-WM-B
Aberdeen Prvg Grd, MD 21005-5066

Dr. Hardev (Dave) Singh
U.S. Army TACOM-ARDEC
Attn: AMSTA-AR-CCL-D
Building 65N
Picatinny Arsenal, NJ 07806

Jack Taylor
ODUSD
Staff Specialist
1777 North Kent
Suite 9030
Rosslyn, VA 22209

Li$_2$NaV$_2$(PO$_4$)$_3$: A 3.7 V Lithium-Insertion Cathode with the Rhombohedral NASICON Structure

Brian L. Cushing and John B. Goodenough[1]

Texas Materials Institute, Mail Code C2201, The University of Texas at Austin, Austin, Texas 78712

Li$_2$NaV$_2$(PO$_4$)$_3$ has been prepared in the rhombohedral NASICON structure via ion exchange from Na$_3$V$_2$(PO$_4$)$_3$. As a lithium-insertion cathode material, Li$_2$NaV$_2$(PO$_4$)$_3$ exhibits a specific discharge capacity of ~ 96 mAh g^{-1} at a current density of 0.50 mA cm^{-2} with a clear plateau near 3.7 V versus lithium metal. Approximately 10% of the capacity is lost through the first 50 cycles, after which the capacity appears to stabilize. During charge and discharge, the Na$^+$ ions tend to remain immobilized in the $A(1)$ site of the NASICON structure, suggesting a direct $A(2) \rightarrow A(2)$ lithium-transport mechanism. © 2001 Academic Press

Key Words: lithium-insertion compounds; battery; lithium-ion; ion-exchange; mixed alkali–ion conduction.

INTRODUCTION

NASICON (for Na$^+$ superionic conductor)-related compounds have been shown to be promising cathode materials for lithium-ion batteries, exhibiting high Li$^+$ mobility and reasonable discharge capacities (1–6). Table 1 details the relevant characteristics of several NASICON-related cathode materials. From Table 1, the transition metals with the most useful redox potentials are Fe^{2+}/Fe^{3+} in a sulfate framework and V^{3+}/V^{4+} in a phosphate framework. Fe$_2$(SO$_4$)$_3$ has already been thoroughly investigated as a cathode material for lithium-ion batteries (2, 3). Here, we report our investigation of the NASICON-related rhombohedral Li$_2$NaV$_2$(PO$_4$)$_3$ as a high-voltage cathode material.

Cursory examination of the NASICON structure reveals its potential as a lithium-insertion cathode. NASICON-related compounds with the highest ionic mobilities possess rhombohedral ($R\bar{3}$) symmetry (7). The $M_2(XO_4)_3$ framework is built of $(XO_4)^{n-}$ ($X = $ Si^{4+}, P^{5+}, S^{6+}, Mo^{6+}, etc.) tetrahedra corner-linked to octahedral-site M^{m+} ($M = $ transition metal) (8). The alkali ions can occupy two different sites. At low alkali content (i.e., $x \le 1$ in $A_xM_2(XO_4)_3$),

an octahedral site, $A(1)$, is selectively occupied (Fig. 1) (8). With $x > 1$, the alkali ions are randomly distributed among the $A(1)$ and three 8-coordinate sites, $A(2)$. The open, 3D nature of the structure allows easy migration of the alkali ions between $A(1)$ and $A(2)$, and the exceptional ionic mobility of the alkali ions is well documented (7).

A NASICON phase, Li$_3$V$_2$(PO$_4$)$_3$, has been previously investigated as a cathode material in lithium batteries (9,10). Like many NASICON-related compounds, however, Li$_3$V$_2$(PO$_4$)$_3$ prepared by direct reaction is not rhombohedral. The Li$_3$V$_2$(PO$_4$)$_3$ phases previously investigated assume the monoclinic ($P2_1/n$) and orthorhombic NASICON structures. The compounds give discharge capacities approaching 131 mAh g^{-1}, but they also exhibit multiple plateaus in their discharge curves (at 4.1, 3.7, and 3.6 V). Furthermore, previous studies have demonstrated that the monoclinic NASICON modification exhibits reduced alkali-ion mobility relative to the rhombohedral form (6,7). While Li$_3$V$_2$(PO$_4$)$_3$ apparently cannot be prepared in the rhombohedral NASICON structure by direct reaction, rhombohedral Na$_3$V$_2$(PO$_4$)$_3$ has been reported (11) and thus provides a suitable starting material for a topotactic ion exchange of Li$^+$ for Na$^+$.

EXPERIMENTAL

Li$_2$NaV$_2$(PO$_4$)$_3$ was prepared via ion exchange from Na$_3$V$_2$(PO$_4$)$_3$. Na$_3$V$_2$(PO$_4$)$_3$ was prepared by direct reaction of NaPO$_3$ (prepared by dehydration of NaH$_2$PO$_4$ (GFS, 99%)) and V$_2$O$_3$ (Aldrich, 99%) in a 3:1 molar ratio. The reactants were ground under acetone with an agate mortar and pestle. After drying, the mixture was placed in an alumina boat and heated at 1°C min^{-1} to 900°C under a 10% H$_2$/Ar mixture flowing at ~ 25 mL min^{-1}. The sample was held at 900°C for 2 days and slowly cooled to room temperature by turning off the furnace. The product was ground under 5% H$_2$SO$_4$ to remove any unreacted phosphates, collected by vacuum filtration, and dried at 150°C in air.

[1] To whom correspondence should be addressed.

TABLE 1
Lithium-Insertion Properties of Selected NASICON-Type Compounds

Compound (Ref.)	Structure type[a]	Redox couple	Redox potential (V)	Number of Li^+ atoms inserted	Reversible discharge capacity $(mAh\,g^{-1})^b$ and current $(mA\,cm^{-2})$
$Fe_2(SO_4)_3$ (2)	R	Fe^{3+}/Fe^{2+}	3.6	2	134 @ 0.015
	M	Fe^{3+}/Fe^{2+}	3.6	2	134 @ 0.015
$V_2(SO_4)_3$ (4)	R	V^{3+}/V^{2+}	2.6	1.8	130 @ 0.5
$LiTi_2(PO_4)_3$ (5)	R	Ti^{4+}/Ti^{3+}	2.5	2.3	160 @ 0.05
				1.5	110 @ 0.5
				1.2	80 @ 1.0
$Li_{3-x}Fe_2(PO_4)_3$ (2,6)	M	Fe^{3+}/Fe^{2+}	2.8	1.6	105 @ 0.05
				1.1	75 @ 0.5
				0.75	55 @ 1.0
$Li_{3-x}FeV(PO_4)_3$ (2)	M	V^{4+}/V^{3+}	3.8	1.6	110 @ 0.075
		V^{3+}/V^{2+}	1.75		
		Fe^{3+}/Fe^{2+}	2.8		

[a] R = rhombohedral form (space group $R\bar{3}$ or $R\bar{3}c$); M = monoclinic form (space group $P2_1/n$).

[b] Discharge capacity given by $[(nF)/(3.6M_w)]$, n = no. of Li^+ atoms inserted per formula unit, F = Faraday's constant $(96,485\,C\,mol^{-1})$, M_w = molecular weight of fully intercalated compound.

Ion exchange of $Na_3V_2(PO_4)_3$ was carried out in an aqueous solution containing a 100% molar excess of $LiNO_3$ (GFS, 99.9%) at $\sim 40°C$. The NASICON phase was stirred in the nitrate solution overnight, collected by vacuum filtration, and washed with deionized water. The process was twice repeated to ensure maximal Li^+ for Na^+ ion exchange.

Powder X-ray diffraction (XRD) studies were performed on a Philips diffractometer equipped with a $CuK\alpha$ radiation source ($\lambda = 1.5406$ Å). Finely divided silicon powder (Aldrich, 99.999%) was used as an internal standard. Peak locations and intensities were determined with the JADE software program using a least-squares method (12).
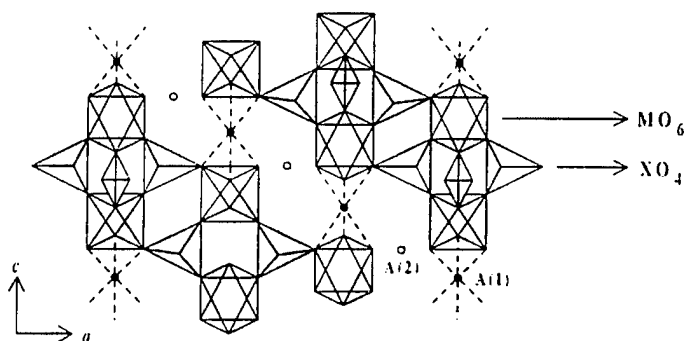

FIG. 1. Idealized representation of the rhombohedral form of the NASICON structure.

Quantitative elemental analysis of lithium was carried out on a Perkin-Elmer 1100 Atomic Absorption Spectrometer (AAS). Samples for AAS were digested in concentrated HNO_3. Quantitative determinations of vanadium were made by potentiometric titrations. Samples for titration were digested in concentrated H_2SO_4. A slight excess of 0.1 M $KMnO_4$ was added to preliminarily oxidize V^{3+} to the pervanadyl ion, VO_2^+. The remaining permanganate was reduced by the addition of sodium nitrite, which was subsequently destroyed by the addition of urea. The VO_2^+ was then potentiometrically titrated with standard ferrous ammonium sulfate solution. The potentiometric equivalence points were determined by the method of Gran (13).

Electrochemical lithium insertion/extraction was investigated by incorporating $Li_2NaV_2(PO_4)_3$ as cathode materials in lithium-ion button cells (type 2320). The NASICON phase was combined in a 70:25:5 proportion with acetylene black to improve conductivity and polytetrafluoroethylene (PTFE) as a binder. The resulting mixture was rolled into a thin sheet from which 1 cm^2 cathode discs of uniform thickness were cut. Cell assembly was carried out in an argon-filled glove box. A 1 M solution of $LiClO_4$ in a 50/50 mixture of propylene carbonate and dimethoxyethane composed the electrolyte. For the button cells, Celgard 2500 served as the separator. The cells were cycled between 2.5 and 4.1 V at 0.50, 1.0, and 2.0 $mA\,cm^{-2}$ against a lithium metal anode on an Arbin BT2043 Battery Test System.

Chemical sodium extraction from $Na_3V_2(PO_4)_3$ was performed by oxidative deintercalation. The NASICON phase was suspended in acetonitrile under inert atmosphere and a 100% molar excess of 1 M NO_2PF_6 in acetonitrile was added with standard Schlenk techniques. The mixture was stirred at room temperature for two days under an inert atmosphere. The product was collected by vacuum filtration, washed with acetonitrile, and dried under vacuum.

RESULTS AND DISCUSSION

$Li_2NaV_2(PO_4)_3$ was obtained via ion exchange of the sodium analogue. Consistent with the findings of others (14), $Na_3V_2(PO_4)_3$ decomposed in molten $LiNO_3$, necessitating that the ion exchange take place in solution at relatively low temperature. During the exchange process, a faint blue coloration of the solution was observed, indicating partial dissolution of the sample. At temperatures above 40°C, the sample dissolution became excessive. Quantitative elemental analysis revealed a final composition of $Li_{1.98}Na_{1.02}V_2(PO_4)_3$, referred to here as $Li_2NaV_2(PO_4)_3$ (Table 2).

Whereas Gopalakrishnan and Kasthuri Rangan (15) reported complete extraction of Na^+, we could not oxidatively extract all the Na^+ from $Na_3V_2(PO_4)_3$; the composition of our deintercalated product was $Na_{0.99}V_2(PO_4)_3$. This may reflect differences in the experi-

TABLE 2
Elemental Analysis Results for $A_xV_2(PO_4)_3$

Compound	% Li [expected]	% Na [expected]	% V [expected]	Experimental composition
Na$_3$V$_2$(PO$_4$)$_3$ (starting material)	—	15.15(4) [15.13]	22.34(5) [22.35]	Na$_{3.00}$V$_{2.00}$(PO$_4$)$_3$
Li$_2$NaV$_2$(PO$_4$)$_3$ (Exchange product)	3.24(2) [3.28]	5.53(3) [5.43]	24.03(4) [24.05]	Li$_{1.98}$Na$_{1.02}$V$_{2.00}$ (PO$_4$)$_3$
NaV$_2$(PO$_4$)$_3$ (Deintercalation product)	—	5.56(2) [5.61]	24.88(3) [24.86]	Na$_{0.99}$V$_{2.00}$(PO$_4$)$_3$

mental methods, as we used NO$_2$PF$_6$ as an oxidizing agent as opposed to chlorine gas.

The XRD results for Li$_2$NaV$_2$(PO$_4$)$_3$ indicate that Li$_2$NaV$_2$(PO$_4$)$_3$ retains the rhombohedral NASICON structure of its precursor (Tables 3, 4; Fig. 2). The XRD results reveal a substantial contraction of the a parameter and expansion of the c parameter of the rhombohedral NASICON unit cell as Na$^+$ is replaced by Li$^+$. This is consistent with the behavior of other NASICON compounds such as Na$_3$Fe$_2$(PO$_4$)$_3$ during Li$^+$ for Na$^+$ ion exchange (6, 16). Those authors attributed the changes to a redistribution of the alkali ions away from $A(1)$ such that some or all of the $A(1)$ sites are left vacant, which introduces a strong electrostatic repulsion along the c axis across the $A(1)$ site. Delmas et al. have demonstrated with neutron diffraction experiments that the exceptional lithium ion conductivity of Li$_{1+x}$Ti$_2$(PO$_4$)$_3$ is due in part to the tendency of Li$^+$ to migrate out of $A(1)$ to $A(2)$ (5). Thus, it would appear that the Li$^+$ cation has a preference for the $A(2)$ site. There is no evidence, however, to indicate a similar behavior for Na$^+$, and in the case of Li$_2$NaV$_2$(PO$_4$)$_3$, Na$^+$ may selectively occupy $A(1)$; otherwise, the Na$^+$ ion should have exchanged for Li$^+$ during the ion-exchange process. Li$^+$ is

too small to coordinate at the center of a large, eight-coordinate cavity like $A(2)$; if Li$^+$ is displaced from the center of the cavity, the electrostatic attraction between Li$^+$ and O^{2-} could easily account for the changes in the c/a ratio.

Cathode performance. The initial charging of the electrochemical cells results in the oxidation of V^{3+} to V^{4+} as 1.8 lithium atoms per formula unit are extracted at ∼ 3.9 V versus lithium. The subsequent discharge produced a single, flat discharge plateau at 3.7 V (Fig. 3). This value is to be compared with 3.8 V for the V^{3+}/V^{4+} couple found for Li$_{3-x}$FeV(PO$_4$)$_3$ (see Table 1). Replacement of one Li$^+$ ion by Na$^+$ has little influence on the energy of the V^{3+}/V^{4+} couple; the dominant influence is the acidity of the polyanion (1–3). At a current density of 0.50 mA cm^{-2}, the initial discharge capacity was 96 mAh g^{-1}, corresponding to the insertion of 1.5 lithium atoms per formula unit. Consistent with the performance of other NASICON-structured cathodes listed in Table 1, the discharge capacity was diminished by increasing the current density (Fig. 4); the capacity, however, recovered when the current was lowered back to 0.50 mA cm^{-2}. This is indicative of a kinetically slow Li$^+$ diffusion process arising from the poor electronic conductivity of the NASICON cathode material. Regardless of
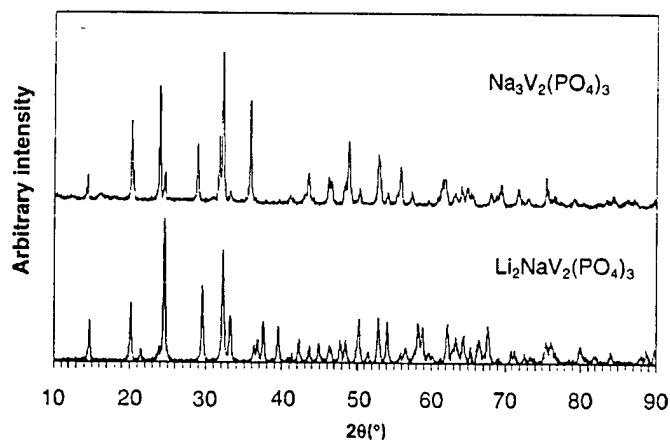
FIG. 2. XRD patterns of Na$_3$V$_2$(PO$_4$)$_3$ and Li$_2$NaV$_2$(PO$_4$)$_3$.

TABLE 3
Summary of Calculated Unit Cells for $A_xV_2(PO_4)_3$

Composition	Calculated unit cell	Literature unit cell
Na$_3$V$_2$(PO$_4$)$_3$	[Hexagonal] a = 8.642(9) Å c = 21.72(3) V = 1405(5) Å^3	[Hexagonal] (11) a = 8.67(2) Å c = 21.71(3) V = 1413(9) Å^3
Li$_2$NaV$_2$(PO$_4$)$_3$	[Hexagonal] a = 8.325(2) c = 22.491(6) V = 1350(2)	This work

Appendix A

TABLE 4
XRD Results and Indexing for $Li_2NaV_2(PO_4)_3$

h	k	l	d_{obs} (Å)	d_{calc} (Å)	I/I_o
1	0	2	6.0758	6.0695	15
1	0	4	4.4457	4.4338	32
1	1	0	4.1611	4.1625	12
0	0	6	3.7492	3.7485	17
1	1	3	3.6440	3.6392	100
2	0	4	3.0350	3.0347	48
1	1	6	2.7866	2.7855	77
2	1	1	2.7077	2.7052	33
2	1	4	2.4519	2.4522	14
2	0	7	2.3998	2.3986	27
3	0	3	2.2867	2.2885	25
1	1	9	2.1437	2.1425	14
2	1	7	2.0788	2.0782	4
2	2	1	2.0721	2.0724	4
3	0	6	2.0232	2.0232	15
2	1	8	1.9563	1.9570	8
1	0	10	1.9073	1.9082	6
3	1	4	1.8822	1.8840	12
3	0	8	1.8253	1.8268	9
2	2	6	1.8177	1.8196	22
4	0	2	1.7809	1.7797	4
2	1	10	1.7337	1.7346	33
3	1	7	1.6968	1.6977	23
3	2	1	1.6472	1.6496	2
4	0	6	1.6241	1.6244	6
2	2	9	1.6006	1.5993	8
3	2	4	1.5873	1.5868	1
4	0	7	1.5713	1.5720	17
1	0	14	1.5656	1.5680	2
4	1	3	1.5404	1.5398	5
3	1	10	1.4929	1.4944	25
3	2	7	1.4727	1.4706	1
2	0	14	1.4668	1.4674	26
4	1	6	1.4497	1.4507	19
3	2	8	1.4274	1.4256	5
1	1	15	1.4113	1.4107	6
4	0	10	1.4068	1.4065	14
5	0	4	1.3977	1.3967	< 1
2	1	14	1.3842	1.3839	32
2	2	13	1.3302	1.3304	7
0	0	17	1.3234	1.3230	9
1	1	17	1.2600	1.2608	18
3	3	8	1.2440	1.2442	38
3 1 15,	6 0	1	1.2000	1.1996	17
5	1	8	1.1766	1.1761	7
3	1	16	1.1508	1.1500	8
4	2	12	1.1008	1.1021	7

current density, capacity fade was evident until about the 50th cycle, at which point the capacities appear to stabilize (Fig. 4).

The presence of Na^+ in the cathode material does not lead to cell failure, at least to 100 cycles. Discharge capacity was diminished by about 10% after 50 cycles, but then appeared to stabilize. Previous studies of NASICON cathode materials that contain only Li^+ in the A sites, e.g., $Li_3Fe_2(PO_4)_3$, also indicate early capacity fade (2, 6), but to

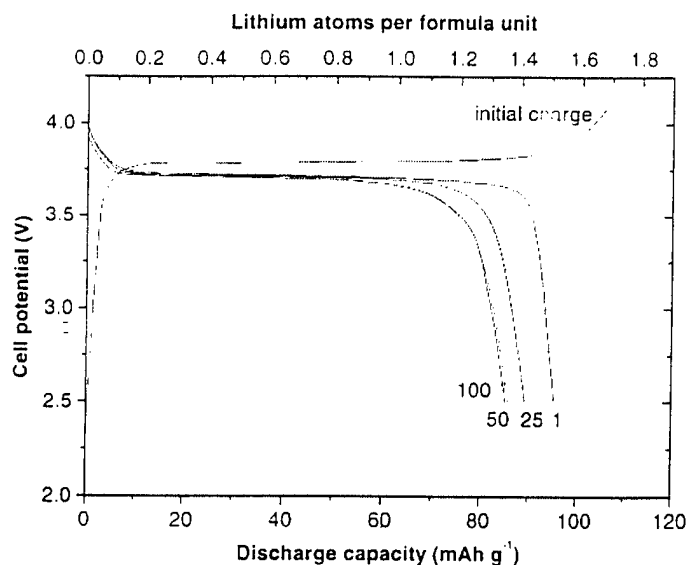**FIG. 3.** Electrochemical insertion/extraction of rhombohedral $Li_2NaV_2(PO_4)_3$ at a current density of $0.50 \, mA \, cm^{-2}$.

our knowledge, the long-term cycle life of these cathode materials has not been investigated.

Ion-transport mechanism. The ion-exchange behavior of $Na_3V_2(PO_4)_3$ suggests that the two Na^+ ions in the $A(2)$ sites are mobile, and thus exchange with Li^+, while the Na^+ in the $A(1)$ site is not. This result is difficult to reconcile with the established ion-transport mechanism of the rhombohedral NASICON structure, which requires a correlated motion involving both $A(1)$ and $A(2)$ sites:
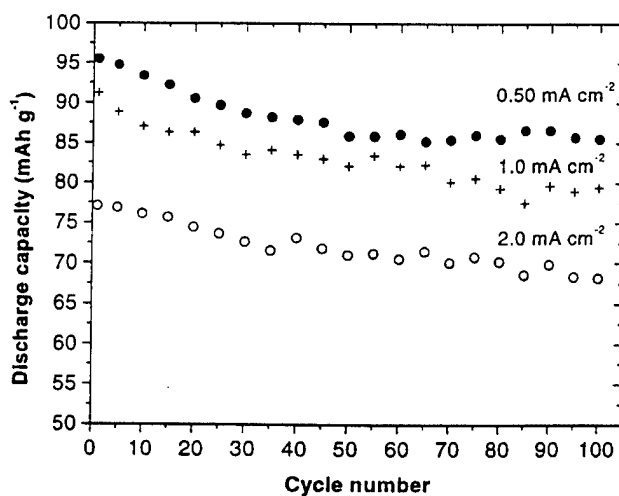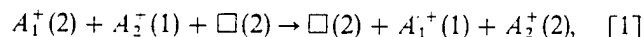
$$A_1^+(2) + A_2^-(1) + \square(2) \to \square(2) + A_1^+(1) + A_2^+(2), \quad [1]$$

FIG. 4. Discharge capacities of rhombohedral $Li_2NaV_2(PO_4)_3$ at various current densities as a function of cycle number.

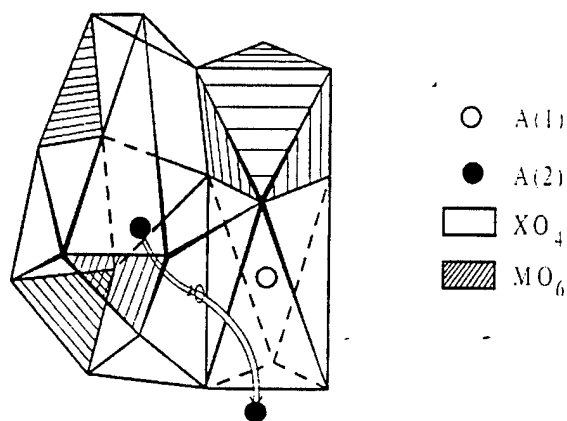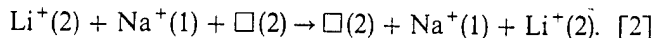**FIG. 5.** Ion transport pathway between adjacent $A(2)$ sites in the rhombohedral NASICON structure.

that a direct $A(2) \rightarrow A(2)$ motion is occurring:

$$Li^+(2) + Na^+(1) + \square(2) \rightarrow \square(2) + Na^+(1) + Li^+(2). \quad [2]$$

Interestingly, the possibility of a direct $A(2) \rightarrow A(2)$ conduction pathway has been previously postulated by others (17–21). Whether the $A(2) \rightarrow A(2)$ mechanism is the prevalent conduction in any rhombohedral NASICON compound is a point of contention, but based solely on the geometric considerations of Li^+ passing through the opening between adjacent $A(2)$ sites, there is no reason to believe that Eq. [2] is not viable (Fig. 5). Mazza has recently demonstrated with bond-valence calculations that in certain circumstances the $A(2) \rightarrow A(2)$ mechanism can be favored (21). The evidence here suggests that this is precisely the situation in $Li_2NaV_2(PO_4)_3$.

CONCLUSIONS

The low-temperature ion exchange of $Na_3V_2(PO_4)_3$ resulted in a mixed-alkali NASICON compound, $Li_2NaV_2(PO_4)_3$. As a lithium-insertion cathode, $Li_2NaV_2(PO_4)_3$ produces a discharge capacity of $96 \, mAh \, g^{-1}$ at $0.50 \, mA \, cm^{-2}$. A 10% capacity fade is evident through the first 50 cycles. The Na^+ ions of $Li_2NaV_2(PO_4)_3$ demonstrate a tendency to remain localized in the $A(1)$ site of the rhombohedral NASICON structure. This compound may represent the first empirical evidence of a NASICONcompound in which a direct $A(2) \rightarrow A(2)$ conduction path way is favored over the usual $A(1) \rightarrow A(2) \rightarrow A(1)$ mechanism.

ACKNOWLEDGMENT

where A represents an alkali ion, the number in parentheses denotes the alkali ion in an $A(1)$ or $A(2)$ site, and $\square$ represents a vacancy (7). Thus, if the Na^+ ions move in a correlated motion between $A(1)$ and $A(2)$, the ions at both sites should be equally capable of being exchanged for Li^+. Likewise, by the mechanism in Eq. [1], both the Na^+ ions situated at $A(1)$ and the Li^+ ions at $A(2)$ of $Li_2NaV_2(PO_4)_3$ should be capable of being extracted from the structure upon electrochemical charging.

To verify whether the Na^+ ions were indeed stationary, the button cells used in the Li^+ insertion/extraction experiments were recharged and opened after completion of their 100th cycle and the Na:V ratio in the cathode materials was determined by quantitative elemental analysis. After 100 cycles, 25% of the Na^+ ions remained in the cathode material. The Na^+ ions that transport out of the NASICON cathode most likely do so while the vanadium is in a mixed III/IV oxidation state, i.e., when $0 < x < 2$ in $Li_xNaV_2(PO_4)_3$. At $x = 0$, only $A(1)$ is occupied and a Na^+ ion in that site tends to be immobilized (7). The $x = 2$ condition was realized during the ion-exchange process, yet the Na^+ in $A(1)$ clearly did not transport. For the bulk of the time during the charge and discharge processes, the NASICON cathode material exists between the $x = 0$ and $x = 2$ end members, when vanadium is present in varying concentrations of V^{3+} and V^{4+}. It seems plausible, then, that the oxidation of vanadium to V^{4+} and the corresponding contraction of its ionic radius introduces a structural distortion to the NASICON framework that reduces the energy difference between $A(1)$ and $A(2)$ and thereby lowers the activation energy of the $A(1) \rightarrow A(2)$ transport pathway.

Notwithstanding the means by which Na^+ eventually escapes $A(1)$, the ion-exchange behavior of $Na_3V_2(PO_4)_3$ and the charge/discharge results of $Li_2NaV_2(PO_4)_3$ strongly suggest that Eq. [1] is not the primary ionic transport pathway of this NASICON compound. One possibility is

REFERENCES

1. A. Manthiram and J. B. Goodenough, *J. Power Sources* **26,** 403 (1989).
2. K. S. Nanjundaswamy, A. K. Padhi, J. B. Goodenough, S. Okada, H. Ohtsuka, H. Arai, and J. Yamaki, *Solid State Ionics* **92,** 1 (1996).
3. A. K. Padhi, V. Manivannan, and J. B. Goodenough, *J. Electrochem. Soc.* **145,** 1518 (1998).
4. J. Gaubicher, J. Angenaut, Y. Chabre, T. Le Mercier, and M. Quarton, *Mol. Cryst. Liq. Cryst.* **311,** 45 (1998).
5. C. Delmas, A. Nadiri, and J. L. Soubeyroux, *Solid State Ionics* **28–30,** 419 (1988).
6. C. Masquelier, A. K. Padhi, K. S. Nanjundaswamy, and J. B. Goodenough, *J. Solid State Chem.* **135,** 228 (1998).
7. J. B. Goodenough, H. Y.-P. Hong, and J. A. Kafalas, *Mater. Res. Bull.* **11,** 203 (1976).
8. H. Y-P. Hong, *Mater. Res. Bull.* **11,** 173 (1976).

9. H. Ohkawa, K. Yoshida, M. Saito, K. Uematsu, K. Toda, and M. Sato, *Chem. Lett.* 1017 (1999).

10. Barker and M. Y. Saidi, U.S. Patent 5, 871, 866,(1999).

11. C. Delmas, R. Olazcuaga, F. Cherkaoui, R. Brochu, and G. Le Flem, *C. R. Acad. Sci. Paris Ser. C* **287**, 169 (1978).

12. JADE. Materials Data Inc., Livermore, CA (2000).

13. G. Gran, *Analyst* **77**, 661 (1952).

14. A. K. Padhi, "Mapping Redox Energies of Electrode Materials for Lithium Batteries," Ph.D. Dissertation. University of Texas at Austin, Austin, Texas, 1997.

15. J. Gopalakrishnan and K. Kasthuri Rangan, *Chem. Mater.* **4**, 745 (1992).

16. C. Masquelier, C. Wurm, J. Rodríguez-Carvajal, J. Gaubicher, and L. Nazar, *Chem. Mater.* **12**, 525 (2000).

17. E. R. Losilla, M. A. G. Aranda, S. Bruque, M. A. Paris, J. Sanz, and A. R. West, *Chem. Mater.* **10**, 665 (1998).

18. D. Tran Qui, J. J. Capponi, M. Gondrand, M. Saïb, J. C. Joubert, and R. D. Shannon, *Solid State Ionics* **3/4**, 219 (1981).

19. M. A. Subramanian, P. R. Rudolf, and A. Clearfield, *J. Solid State Chem.* **60**, 172 (1985).

20. F. Cherkaoui, G. Villeneuve, C. Delmas, and P. Hagenmuller, *J. Solid State Chem.* **65**, 293 (1986).

21. D. Mazza, *J. Solid State Chem.* **156**, 154 (2001).